

# Fabrication of Organic Thin Film Transistors using Inkjet Printing of PEDOT:PSS

Sourajit Das, Akshaya Venkatakrishnan, Hiromichi Yamamoto and Pat Watson<sup>1, a)</sup>

<sup>1</sup>*Singh Center for Nanotechnology, University of Pennsylvania  
3205 Walnut St. Philadelphia, PA 19104*

(Dated: Received 29 August 2018; accepted 13 November 2019)

An Organic Thin Film Transistors (OTFT) using poly(3,4-ethylene dioxythiophene) polystyrene sulfonate (PEDOT:PSS) is fabricated using a Fujifilm Dimatix Inkjet printer, and successfully shows the field effect transistor characteristics as a result of optimization of the inkjet printing condition. The V-I characteristics of the two devices also satisfy the fundamental property of transistors that wider is the channel length, smaller is the drain current. Another significant property is observed that the higher gate voltage induces the higher drain current as it allows larger carrier concentration in the channel region.

Key Words: OTFT, inkjet printing, PEDOT:PSS, V-I characteristics

## I. Introduction

Since the advent of Organic Field Effect Transistor (OFET) or Organic Thin Film Transistor (OTFT)<sup>1</sup>, the OTFT has been the potential candidate of low-cost, large-area, and flexible electronic devices where inorganic devices are a failure. The applications utilize the intrinsic characteristics of organic semiconductors such as mechanical flexibility, low-temperature processing and high-throughput manufacturing at low costs.<sup>2,3</sup> Various fabrication techniques have also been studied to develop the OTFTs with high carrier mobility by introducing additional source/drain contact materials, using appropriate dielectrics and optimizing the organic semiconductor deposition conditions. Some of ongoing works are using Pentacene, poly(3,4-ethylene dioxythiophene)-poly(styrene sulfonate) (PEDOT:PSS),<sup>4</sup> Poly(3-hexylthiophene-2,5-diyl) (P3HT) etc. as the organic semiconductors.

On the other hand, the deposition of organic semiconductors plays a vital role in deciding the electrical properties of a transistors. In the beginning of OTFT, an organic material was electropolymerized or simply spin coated on the substrate. The organic layer was eventually patterned using Nano imprint lithography (NIL), optical lithography, and shadow masking.<sup>5</sup> Inkjet printing, called as digital writing technique, is another technique to place the "ink" at the desired location in a micron scale without a mask.

In this study, Dimatix inkjet printer (Fujifilm) shown in Fig.1 has been used to deposit the PEDOT:PSS layer between the drain and the source regions,<sup>6,7</sup> and the optimization of the inkjet printing is described. The print-

ability and the electrical characterization of PEDOT:PSS are also discussed later.



FIG. 1. The Dimatix Inkjet Printer.

## II. Experimental Procedure

The preliminary steps of fabricating the OTFT began by creating a shadow mask for the device. The mask was carved out from a stainless steel shim using IPG IX280-DXF Green Laser Micromachining tool. Figure 2 shows the mask designed to fabricate five sets of OTFTs, and the sets have the drain and source with the channel lengths of 100, 250, 500, and 1000  $\mu\text{m}$  between them. The width of the channel was set at 500  $\mu\text{m}$ . Figure 3 delineates the overall core process of fabricating the OTFTs.

### A. Deposition of Silicon Dioxide

Approximately 100 nm thick silicon dioxide film was deposited onto a 4 inch silicon wafer using either of Oxford PlasmaLab 100 Plasma Enhanced Chemical Vapor Deposition (PECVD) or Sandvik Oxidation furnace where the oxide layer was thermally grown on a silicon

<sup>a)</sup>Electronic mail: gewatson@seas.upenn.edu

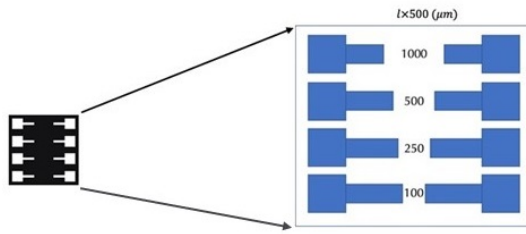


FIG. 2. The mask used for fabricating the OTFT. The length is varied here, keeping the width fixed.

wafer. Both the methods were experimented for the fabrication of OTFTs.

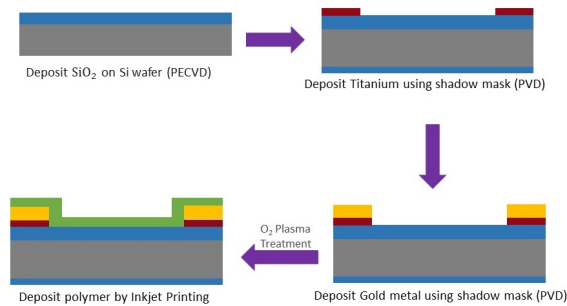


FIG. 3. Process flow of OTFT fabrication.

### B. Deposition of source and drain

Approximately 10 nm thick titanium film was e-beam evaporated as an adhesion layer through the shadow mask, followed by depositing 150 nm thick gold film, using Kurt Lesker PVD 75, to define the drain and source regions. The device was then treated with an oxygen plasma for 1 min using Anatech SCE-108 Barrel Asher to facilitate the wetting of the PEDOT:PSS aqueous ink to the oxide surface.

### C. Deposition of organic polymer

The ink cartridges with a reservoir of 10 pL were used in the study. The PEDOT:PSS solution (2.8 wt% dispersion in  $H_2O$ , low-conductivity grade) was purchased from Sigma-Aldrich, and was mixed with diethylene glycol to adjust the viscosity, as described later. Diethylene glycol was purchased from Sigma-Aldrich, and was used as received. The mixed ink was injected into the ink cartridge through a  $0.5 \mu m$  filter using the syringe. Once the cartridges were ready, it was installed in the printer with a desired head angle to achieve corresponding drop spacing. The ink was inkjet printed with a single nozzle according to the desired length of the channel between the drain and the source.

## III. Results and Discussion

### A. Optimization of print parameters

When the surface of the silicon dioxide was hydrophobic, the aqueous ink did not stick well to the channel regions. Thus the device had to be treated with an oxygen plasma to make the surface "clean" or hydrophilic before inkjet printing of the PEDOT:PSS ink. Furthermore, when the PEDOT:PSS ink purchased was used directly as the ink, the nozzles of the cartridge was clogged because of its high viscosity and higher surface tension of the ink. Hence the viscosity of the ink was reduced by mixing it with diethylene glycol as the solvent.

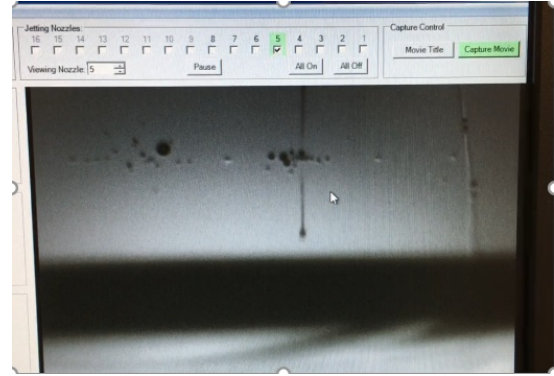


FIG. 4. PEDOT:PSS ink jetting out of the nozzle of a 10 pL cartridge

The inkjet printing of the PEDOT:PSS solution required optimization of various parameters before it was ready to print the organic channel. The optimization of the parameters was carried out using the Drop Watcher of the printer. Figure 4 shows the smooth jetting of PEDOT:PSS ink from the nozzles of a cartridge when the parameters were optimized. Table I indicates the range of operating as well as optimized parameters for inkjet printing of the PEDOT:PSS ink. Table II in Appendix A shows the effects of variation of drop spacing or corresponding sabre angle on the print pattern and quality. The optimization process started with considering a set of parameters randomly and tuning every parameter till the ink could jet out of the nozzles smoothly. Once the organic polymers were deposited, the device was then baked on a hot plate at  $60^\circ C$  for about 30 min. The PEDOT:PSS became transparent after the solvent diethylene glycol dries out, as can be seen in Fig.5.

### B. V-I Characterization

8 devices prepared were assessed in terms of voltage-current (V-I) characteristics, but some of them indicated poor performance. Figure 6 shows the V-I characteristics of the two devices of PEDOT:PSS TFT, device "3" and "4". The drain current was measure by varying the voltage between the drain and source ( $V_{GS}$ ) from 0V to 25V, while keeping the gate voltage ( $V_G$ ) constant. The gate voltage was varied for three different values to get three different curves. The distance between the drain

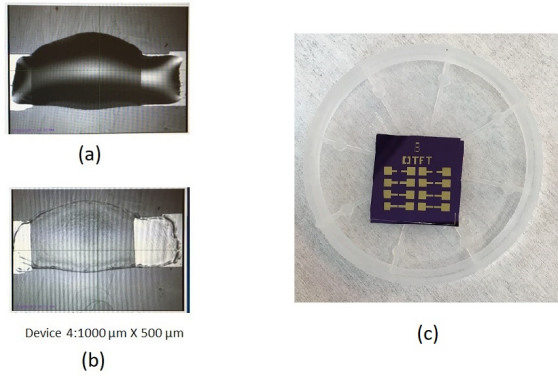


FIG. 5. (a) Sample result of Device 4 after inkjet printing (b) Result of baking the Device 4 after inkjet printing (c) The device consisting of the 8 OTFTs

TABLE I. Operating and optimized parameters for inkjet printing of PEDOT:PSS.

Critical Parameters	Typical range	Optimal value
Ink : Solvent Ratio	1:0, 1:1, 1:2, 1:3	1:2
Cartridge Temperature ( $^{\circ}\text{C}$ )	30, 40, 50, 55	50
Cartridge Voltage (V)	15 - 32	31
Jetting Frequency (KHz)	1 - 6	5
Number of nozzles & position	5 - 14	10
Platen Temperature ( $^{\circ}\text{C}$ )	40, 50	40
Head angle ( $^{\circ}$ )	2.3 - 28.2	3.4
Drop Spacing ( $\mu\text{m}$ )	10 - 120	15

and source of Device "3R" was  $250 \mu\text{m}$ , while that of Device "4L" was  $100 \mu\text{m}$ . As shown in Figure 6, the drain current of  $250 \mu\text{m}$  gap device "3R" for the gate voltage of 15 V is approximately  $70 \mu\text{A}$  in the saturation region, whereas the drain current of  $100 \mu\text{m}$  gap device "4L" is approximately  $170 \mu\text{A}$  in the saturation region. This indicates that a narrow channel length allows higher drain current for a given gate-source voltage because charge carriers reach the drain faster. Furthermore, the drain current increases with increase in the gate voltage.

Two sets of devices were also fabricated using the same mask. Figure 7 shows (a) one of the set fabricated without using optimized print parameters and (b) the other set fabricated using optimized printing techniques. As can be seen in Figure 7, the device fabricated using optimized printing parameters shows 20 times more drain current than the devices fabricated without using optimized printing parameters, indicating that TFT property is seriously affected by the printing condition.

#### IV. Summary

The OTFT of PEDOT:PSS has been fabricated using Dimatix Inkjet printer, and has successfully shown the field effect transistor property. The V-I characteristics of the two devices also satisfy the fundamental property of

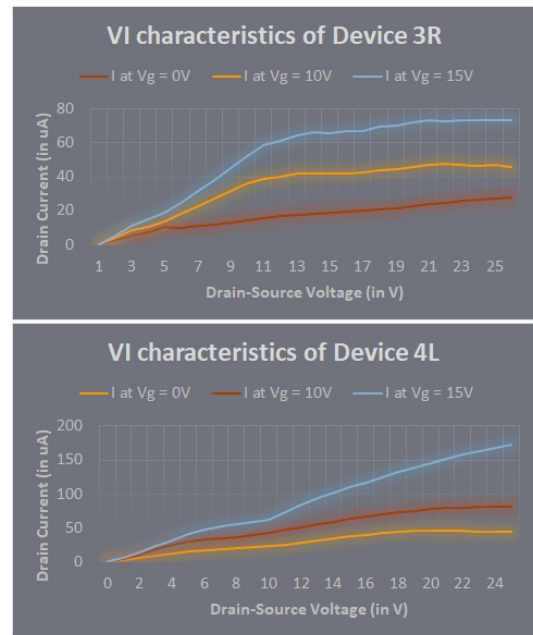
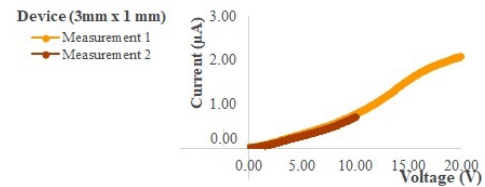
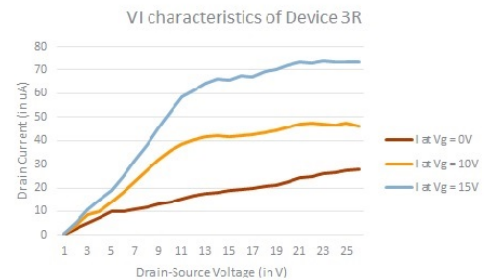


FIG. 6. VI characteristics of Device "3" and Device "4"



(a)



(b)

FIG. 7. Comparison of VI characteristics of a sample device before and after optimization of parameters

transistors that the smaller is the channel length, larger is the drain current. Another significant property is observed that the higher gate voltage induces the higher drain current as it increases the carrier concentration in the channel region.

Further works will be carried out using different ink

such as P3HT (Poly(3-hexylthiophene-2,5-diyl)), TIS Pentacene (6,13-Bis(triisopropylsilylethynyl)pentacene) and modifying the device features to obtain better results. Further results on evaluation of carrier mobility will be presented in the upcoming article.

## V. Acknowledgements

This work was performed at the Singh Center for Nanotechnology at the University of Pennsylvania, a member of the National Nanotechnology Coordinated Infrastructure (NNCI) network, which is supported by the National Science Foundation (Grant NNCI-1542153).

<sup>1</sup>Koezuka H. Ando T. Tumura, A. Macromolecular electronic device: Field-effect transistor with a polythiophene thin film. *Applied Physics Letters*, 49(18):1210–1212, 1986.

<sup>2</sup>Tracy Y. Chang, Vikramaditya G. Yadav, Sarah De Leo, Agustin Mohedas, Bimal Rajalingam, Chia-Ling Chen, Selvapraba Selvarasah, Mehmet R. Dokmeci, and Ali Khademhosseini. Cell and protein compatibility of parylene-c surfaces. *Langmuir*, 23(23):11718–11725, 2007. PMID: 17915896.

<sup>3</sup>Davi H. Starnini de Camargo Carlos C. Bof Bufon Kleyton Torikai, Rafael Furlan de Oliveira. Low-voltage, flexible, and self-encapsulated ultracompact organic thin-film transistors based on nanomembranes. *Nano Letters*, 18(9):5552–5561, 2018.

<sup>4</sup>Demetrio A. da Silva Filho Jean-Luc Brédas Paul C. Ewbank Kent R. Mann Christopher R. Newman, C. Daniel Frisbie. Introduction to organic thin film transistors and design of n-channel organic semiconductors. *Chemistry of Materials*, 16(23):4436–4451, 2004.

<sup>5</sup>Jun-Yu Chen Henry J.H.Chen, Yen-Bang Liu. Fabrication of organic thin film transistors with the nano-groove al gate electrodes by using uv nano imprint technology. *Microelectronic Engineering*, 98:155–158, 2012.

<sup>6</sup>Yongan bu-Ningbin Wang Xiao Mei Xiong You Lun Yin, Zhou Ping Huang. Inkjet printing for flexible electronics: Materials, processes and equipments. *Chinese Science Bulletin*, 55:3383–3407, 2010.

<sup>7</sup>Thomas Baumann Reinhard Sridhar Ashok, Blaudeck. Inkjet printing as a key enabling technology for printed electronics. *Material Matters*, 6:12–15, 2011.

## A. Appendix A

The raw data for all the results obtained for different drop spacings and corresponding head/sabre angles are shown in Table II. Other conditions are set to be the optimal values indicated in Table I. Here the print quality is defined optimal when the printing is good as well as the aggregation of the drops is obtained in a uniform pattern.

TABLE II. Results of variation of drop spacing. Other conditions are set to be the optimal values indicated in Table I.

Number	Sabre angle (°)	Drop Spacing ( $\mu m$ )	Print quality
1	120	28.2	Good but no aggregation of drops
2	115	26.9	Good but no aggregation of drops
3	110	25.7	Good but no aggregation of drops
4	105	24.4	Good but no aggregation of drops
5	100	23.2	Good but no aggregation of drops
6	95	22.0	Good but no aggregation of drops
7	90	20.8	Good but no aggregation of drops
8	85	19.6	Good but no aggregation of drops
9	80	18.4	Good but no aggregation of drops
10	75	17.2	Good but no aggregation of drops
11	70	16.0	Good but no aggregation of drops
12	65	14.8	Good but no aggregation of drops
13	60	13.7	Good but no aggregation of drops
14	55	12.5	Good but no aggregation of drops
15	50	11.4	Good but no aggregation of drops
16	45	10.2	Good but no aggregation of drops
17	40	9.1	Good but no aggregation of drops
18	35	7.9	Good but no aggregation of drops
19	30	6.8	Good but no aggregation of drops
20	25	5.6	Good but no aggregation of drops
21	20	4.5	Good but no aggregation of drops
22	15	3.4	Optimal print shape and size
23	10	2.3	Bad; too much aggregation of drops
24	5	1.1	Bad; too much aggregation of drops